970 *Chem. Mater.* **2011,** *23,* 970–975
DOI:10.1021/cm1025975

CHEMISTRY OF MATERIALS
Article

Simple Formation of C_{60} and C_{60}-Ferrocene Conjugated Monolayers Anchored onto Silicon Oxide with Five Carboxylic Acids and Their Transistor Applications

Yoshimitsu Itoh,*[,†,¶,⊥] Bumjung Kim,[†] Raluca I. Gearba,[‡] Noah J. Tremblay,[†] Ron Pindak,[#] Yutaka Matsuo,[§,¶] Eiichi Nakamura,[§,¶] and Colin Nuckolls[†]

[†]*Deparment of Chemistry and The Center for Electron Transport in Molecular Nanostructures, Columbia University, New York, New York 10027, United States,* [‡]*Center for Functional Nanomaterials, Brookhaven National Laboratory, Upton, New York 11973, United States,* [#]*National Synchrotron Light Source, Brookhaven National Laboratory, Upton, New York 11973, United States,* [§]*Nakamura Functional Carbon Cluster Project, ERATO, Japan Science and Technology Agency, Hongo, Bunkyo-ku, Tokyo, 113-0033, Japan, and* [¶]*Department of Chemistry, The Univeristy of Tokyo, Hongo, Bunkyo-ku, Tokyo, 113-0033, Japan.* [⊥]*Current address of Y. I. Department of Chemistry and Biotechnology, The University of Tokyo, Hongo, Bunkyo-ku, Tokyo, 113-8656, Japan.*

Received September 9, 2010. Revised Manuscript Received December 11, 2010

C_{60} and C_{60}-ferrocene conjugated molecule bearing five carboxylic acids successfully anchor onto a silicon oxide surface as a monolayer through a simple method of simply dipping an amino-terminated surface into the solution of the C_{60} derivatives. The monolayer structure was characterized by UV−vis spectroscopy, X-ray reflectivity, X-ray photoelectron spectroscopy, and IR spectroscopy to reveal that the molecules are standing presenting its C_{60} spherical face at the surface. The electronic effect of the C_{60} monolayer and the ferrocene-functionalized C_{60} monolayer in OFET devices was investigated. When an *n*-type OFET was fabricated on the ferrocene functionalized monolayer, we see an enhancement in the mobility. When a *p*-type OFET was made the ferrocene-functionalized C_{60} monolayer showed a lowering of the carrier mobility.

Introduction

In this study, we investigate self-assembled monolayers (SAMs) of anisotropically functionalized C_{60} molecules, and we explore the feasibility of these SAMs as electrically active materials in field-effect transistors (FETs). C_{60}, also known as buckminsterfullerene,[1] is an attractive material for electronic applications, such as photovoltaics and FETs[2,3] as suggested by its high electron mobilities.[4] Of particular interests are the SAMs[5] of C_{60} showing unique properties and potential for advanced electronic applications.[6] There have been many studies of a monolayer of C_{60} derivatives on gold, ITO, or other substrates.[7] However, compared to the monolayer on gold, there are only a few reports for the formation of fullerene monolayers on silicon oxide surfaces[8] that are important for electronic device applications especially for organic FETs. Moreover, all of these prior studies involve covalent functionalization on silicon oxide surfaces. Some of them make a reaction of C_{60} itself with a nitrogen functional group on the surface,[8b−d,h] which have a possibility for an incomplete reaction of C_{60}, and the others make a reaction utilizing the C_{60} itself or prefunctionalized C_{60} with the surface using a coupling

*To whom correspondence should be addressed. E-mail: itoh@macro.t.u-tokyo.ac.jp.

(1) Kroto, H. W.; Heath, J. R.; O'Brien, S. C.; Curl, R. F.; Smalley, R. E. *Nature* **1985**, *318*, 162–163.
(2) Review: (a) Mirikin, C. A.; Caldwell, W. B. *Tetrahedron* **1996**, *52*, 5113–5130. (b) Konishi, T.; Ikeda, A.; Shinkai, S. *Tetrahedron* **2005**, *61*, 4881–4899. (c) Gludi, D. M.; Illescas, B. M.; Atienza, C. M.; Wielopolski, M.; Martin, N. *Chem. Soc. Rev.* **2009**, *38*, 1587–1597.
(3) (a) Sariciftci, N. S.; Smilowitz, L.; Heeger, A. J.; Wudl, F. *Science* **1992**, *258*, 1474–1476. (b) Yu, G.; Gao, J.; Hummelen, J. C.; Wudl, F.; Heeger, A. J. *Science* **1995**, *270*, 1789–1791. (c) Haddon, R. C.; Perel, A. S.; Morris, R. C.; Palstra, T. T. M.; Hebard, A. F.; Fleming, R. M. *Appl. Phys. Lett.* **1995**, *67*, 121–123.
(4) (a) Priebe, G.; Pietzak, B.; Könenkamp, R. *Appl. Phys. Lett.* **1997**, *71*, 2160–2162. (b) Anthopoulos, T. D.; Ramil, A. M.; Sitter, H.; Cölle, M.; Leeuw, D. M. *Appl. Phys. Lett.* **2006**, *89*, 213504/1–213504/3.
(5) Love, J. C.; Estroff, L. A.; Kriebel, J. K.; Nuzzo, R. G.; Whitesides, G. M. *Chem. Rev.* **2005**, *105*, 1103–1169.
(6) Ma, H.; Yip, H.-L.; Huang, F.; Jen, A. K.-Y. *Adv. Funct. Mater.* **2010**, *20*, 1371–1388.
(7) Examples of C_{60} derivative monolayer; on gold: (a) Shi, X.; Caldwell, W. B.; Chen, K.; Mirkin, C. A. *J. Am. Chem. Soc.* **1994**, *116*, 11598–11599. (b) Imahori, H.; Norieda, H.; Yamada, H.; Nishimura, Y.; Yamazaki, I.; Sakata, Y.; Fukuzumi, S. *J. Am. Chem. Soc.* **2001**, *123*, 100–110. (c) Shirai, Y.; Cheng, L.; Chen, B.; Tour, J. M. *J. Am. Chem. Soc.* **2006**, *128*, 13479–13489. (d) Chen, T.; Pan, G.−B.; Yan, H.−J.; Wan, L.−J.; Matsuo, Y.; Nakamura, E. *J. Phys. Chem. C* **2010**, *114*, 3170–3174. (e) Matsuo, Y.; Lacher, S.; Sakamoto, A.; Matsuo, K.; Nakamura, E. *J. Phys. Chem. C* **2010**, *14*, 17741–17752. On ITO: (f) Yamada, H.; Imahori, H.; Nishimura, Y.; Yamazaki, I.; Ahn, T. K.; Kim, S. K.; Kim, D.; Fukuzumi, S. *J. Am. Chem. Soc.* **2003**, *125*, 9129–9139. (g) Cho, Y.−J.; Ahn, T. K.; Song, H.; Kim, K. S.; Lee, C. Y.; Seo, W. S.; Lee, K.; Kim, S. K.; Kim, D.; Park, J. T. *J. Am. Chem. Soc.* **2005**, *127*, 2380–2381. (h) Matsuo, Y.; Kanaizuka, K.; Matsuo, K.; Zhong, Y.−W.; Nakae, T.; Nakamura, E. *J. Am. Chem. Soc.* **2008**, *130*, 5016–5017. (i) Matsuo, Y.; Ichiki, T.; Radhakrishnan, S. G.; Guldi, D. M.; Nakamura, E. *J. Am. Chem. Soc.* **2010**, *132*, 6342–6348. For other examples, see review: (j) Bonifazi, D.; Enger, O.; Diederich, F. *Chem. Soc. Rev.* **2007**, *36*, 390–414.

 Published on Web 01/13/2011

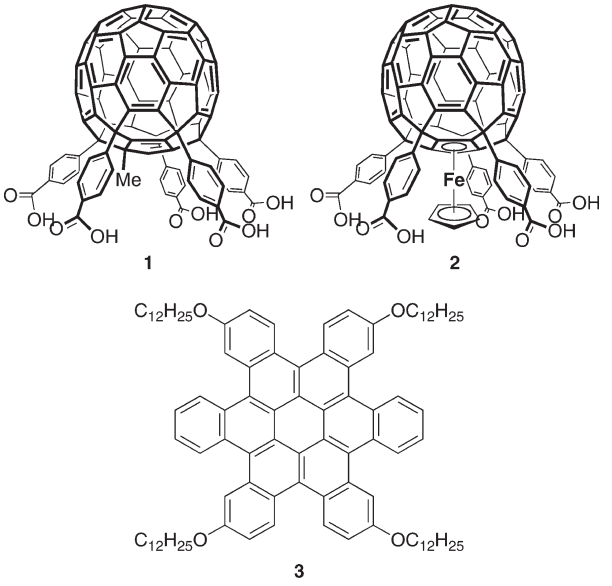

Figure 1. Molecular structure of the C_{60} derivatives **1** and **2** and contorted hexabenzocoronene **3**.

reagent,[8a,e−g,i] which might result in a contamination of the surface. Therefore, it is difficult to avoid making a SiO_2 surface with a nonuniform electronic structure. Here, we suggest a simple way to form monolayers of C_{60} derivatives on silicon oxide surfaces by using SAMs of C_{60} molecules functionalized with five carboxylic acids **1** and **2** (Figure 1). We also demonstrate the usefulness of these SAMs for organic FET applications using the C_{60} molecule itself and contorted hexabenzocoronene (HBC) **3**[9] (Figure 1).

Experimental Section

Materials. The C_{60} derivatives **1** and **2**,[7h,10] and contorted hexabenzocoronene (HBC) derivative **3** (Figure 1)[9] were synthesized according to the reported procedure. Quartz flats for UV−vis spectroscopy were purchased from NSG Precision Cells Inc. Silicon wafers for AFM, X-ray reflectivity, X-ray photoelectron spectroscopy, ATR-IR, and FET fabrication were obtained from Process Specialties Inc. High purity C_{60} (> 99.9%, sublimed) was purchased from Bucky USA.

Monolayer Formation. Silicon oxide surfaces were cleaned by soaking them into CH_2Cl_2 at room temperature for 15 min followed by 20 min in a 1:1:5 = NH_4OH/30% H_2O_2/DI H_2O at 70 °C. Immediately after rinsing in DI H_2O and drying in a steam of N_2 gas, the samples were immersed in a 2 v/v % solution of 3-aminopropyltriethoxysilane (APTES) in ethanol for 25 min at room temperature. Post bake at 120 °C for 5 min gave the monolayer of APTES. The APTES covered samples were then immersed in 0.1 mM solution of **1** (or **2**) in THF for 24 h (30 min for **2**) at room temperature. After the monolayer assembly, the samples were soaked in clean THF for 30 min at room temperature for washing out the unbound molecules.

Surface Characterization. UV−vis spectroscopy was performed using a single-beam Agilent 8453 spectrometer with a modified sample holder. The monolayer was formed on ultrathin quartz flats to reduce background contributions. X-ray reflectivity measurements were performed at the National Synchrotron Light Source on beamline X22A using an X-ray beam of 32 KeV and 15 μm vertical and 1 mm horizontal beam size. The X-ray reflectivity data were fitted using a box-based model having discrete layers corresponding to the Si substrate, native oxide layer, the APTES layer, and C_{60}. The parameters for fitting have been adjusted with a Marquardt−Levenberg least-squares routine. Since the scattering length density (SLD) contrast between the APTES layer and the C_{60} material is low, to avoid the interdependence of the fitting parameters during the fitting procedure, the parameters corresponding to the APTES layer have been obtained from a separate sample without C_{60} and then fixed in the subsequent fit.[11] XPS experiments were performed with a Kratos AXIS-Ultra Spectrometer equipped with a monochromatic Al source operated at 255 W. The pass energy was set to 160 eV for survey spectrun and 20 eV for high resolution scan of N1s. IR spectroscopy was performed by using a N_2-purged Nicolet IR spectrometer with a mercury cadmium tellurium (MCT) detector. Spectra were obtained by using a GATR (Harrick Inc.) total reflectance accessory equipped with a hemispherical germanium crystal.

FET Device Fabrication. Bottom-contact geometry was used in all the transistor devices. A highly *n*-type doped (< 0.005 Ωcm) Si wafer with a 300 nm thermally grown silicon oxide surface was used for electrical measurements. The wafer was cleaned with 70:30 = H_2SO_4/30% H_2O_2 (*Caution: This is called a piranha solution and is an extremely dangerous oxidizing agent. The solution should be handled with care using appropriate shielding.*) for 1 h at 100 °C. Then, source and drain electrodes (5 nm Cr followed by 30 nm Au) were vacuum-deposited through a shadow mask. The resulting channel was (W, L) = (115 μm, 10 μm) for C_{60} transistors and (W, L) = (2 mm, 85 μm) for HBC transistors. The monolayer of **1** and **2** were formed according to the procedure described earlier. C_{60} transistors were then fabricated by thermal evaporation of 50 nm C_{60} on to the substrate at 1.5−1.7 Å/s at $< 10^{-6}$ Torr. HBC transistors were fabricated by spin coating 1 mg/mL solution of **3** in $CHCl_3$ or $(CH_2Cl)_2$ at 1200 rpm for 20 s. The transistor characterization was carried out at room temperature, in Ar atmosphere (C_{60} transistors) or in an ambient atmosphere (HBC transistors) using an Agilent 4155C semiconductor characterization system and a Karl Suss (PM5) manual probestation. The mobility was calculated according to ref 12.

Results and Discussions

A monolayer of **1** was formed on an amine-modified silicon oxide surface. First, a monolayer of 3-aminopropyltriethoxysilane (APTES) was formed on a silicon oxide surface;[13] then, the substrate was immersed into a 0.1 mM

(8) (a) Chupa, J. A.; Xu, S.; Fischetti, R. F.; Strongin, R. M.; McCauley, J. P., Jr.; Smith, A. B., III; Blasie, J. K. *J. Am. Chem. Soc.* **1993**, *115*, 4383–4384. (b) Tsukruk, V. V. *Langmuir* **1994**, *10*, 996–999. (c) Tsukruk, V. V. *Langmuir* **1996**, *12*, 3905–3911. (d) Lee, H.; Jeon, C. *Synth. Met.* **1997**, *86*, 2297–2298. (e) Wei, T.-X.; Zhai, J.; Ge, J.-H.; Gan, L.-B.; Huang, C.-H.; Luo, G.-B.; Ying, L.-M.; Liu, T.-T.; Zhao, X.-S. *Appl. Surf. Sci.* **1999**, *151*, 153–158. (f) Wei, T.-X.; Zhai, J.; Ge, J.; Gan, L.−B.; Huang, C.−H.; Luo, G.−B.; Ying, L.−M. *J. Colloid Interface Sci.* **2000**, *222*, 262–264. (g) Gulino, A.; Bazzano, S.; Condorelli, G. G.; Giuffrida, S.; Mineo, P.; Satriano, C.; Scamporrino, E.; Ventimiglia, G.; Vitalini, D.; Fragalà, I. *Chem. Mater.* **2005**, *17*, 1079–1084. (h) Park, B.; Paoprasert, P.; In, I.; Zwickey, J.; Colavita, P. E.; Hamers, R. J.; Gopalan, P.; Evans, P. G. *Adv. Mater.* **2007**, *19*, 4353–4357. (i) Guérin, D.; Lenfant, S.; Godey, S.; Vuillaume, D. *J. Mater. Chem.* **2010**, *20*, 2680–2690.
(9) Xiao, S.; Myers, M.; Miao, Q.; Sanaur, S.; Pang, K.; Steigerwald, M. L.; Nuckolls, C. *Angew. Chem., Int. Ed.* **2005**, *44*, 7390–7394.
(10) Zhong, Y.-W.; Matsuo, Y.; Nakamura, E. *Org. Lett.* **2006**, *8*, 1463–1466.
(11) Gao, Y.; Tang, Z.; Watkins, E.; Majewski, J.; Wang, H.-L. *Langmuir* **2005**, *21*, 1416–1423.
(12) Miao, Q.; Lefenfeld, M.; Nguyen, T. Q.; Siegrist, T.; Kloc, C.; Nuckolls, C. *Adv. Mater.* **2005**, *17*, 407–412.

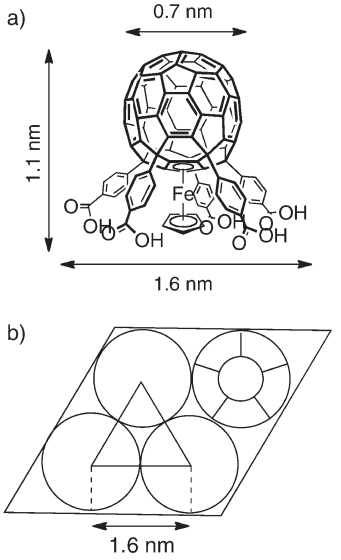

Figure 2. Size information of the compounds **1** and **2**. (a) Molecular size of the molecule **2** according to the X-ray crystallography.[10] (b) Ideal packing of the molecule **1** and **2** on the surface which corresponds to 0.45 molecules/nm^2.

solution of **1** in THF at room temperature for 24 h without any coupling reagent. The coverage on the surface was calculated to be 0.42 molecules/nm^2 from the absorption cross section (5.3×10^{-16} cm^2/molecules in THF solution. See Supporting Information). This value is in good agreement with the calculated value for tightly packed molecules standing upright to the surface (0.45 molecules/nm^2, Figure 2). A monolayer of **2** (coverage = 0.50 molecules/nm^2) was obtained in the same way except that the substrate was immersed in the solution of **2** for 30 min; this was to avoid the formation of multilayer of **2**. AFM images showed that the monolayers were uniform (Figure 3 and Supporting Information Figures S-7 and S-8). Without using an amine-modified surface, the immersion gave only islands of the molecules rather than uniform layers.

Structural analysis of the monolayer was performed using synchrotron X-ray reflectivity, XPS, IR, and UV−vis spectroscopy. From synchrotron X-ray reflectivity, information about the thickness, electron density distribution, and roughness of the monolayers was obtained. Figure 4a shows the reflectivity data corresponding to the layer of **1** together with the fit. The fit was calculated based on a box model having discrete layers corresponding to the Si substrate, native oxide, the APTES layer and the C_{60} derivative **1**. The parameters corresponding to the APTES layer were obtained from a separate sample lacking **1** and were then fixed in the subsequent fit.[11] The corresponding scattering length density (SLD) as a function of the film depth is shown in Figure 4b. This analysis gave thicknesses of 10.9 ± 0.2 Å for **1** and 12.9 ± 0.2 Å for **2** (Supporting Information Table S-1). These numbers agree quite well with the size of

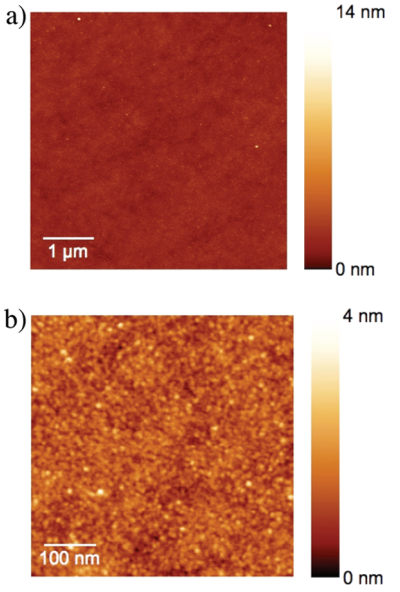

Figure 3. AFM hight image of the monolayer of **1**. rms roughness = 0.49 nm, average height = 1.64 nm. (a) 5 × 5 mm image and (b) 500 × 500 nm image.

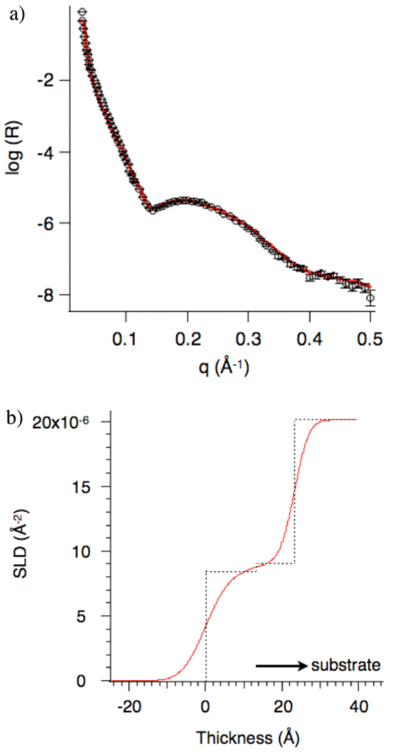

Figure 4. (a) X-ray reflectivity curve corresponding to molecule **1** (black open circles) along with the plot of the data fit (solid red line). (b) Electron density profile (red) obtained from the model along with box diagram (dashed black) illustrating thickness and electron density with roughness equal to zero.

the molecules and indicate the formation of a single monolayer. Surface roughness of the monolayer is 5.0 ± 0.2 Å for **1** and 4.9 ± 0.3 Å for **2**, and these values are in good agreement with the result of AFM (Supporting Information Figure S-5−8).

The XPS spectrum shows that hydrogen bonding is involved in the monolayer formation. Figure 5a is an XPS

(13) (a) Haller, I. *J. Am. Chem. Soc.* **1978**, *100*, 8050–8055. (b) Vandenberg, E. T.; Bertilsson, L.; Liedberg, B.; Uvdal, K.; Erlandsson, R.; Elwing, H.; Lundström, I. *J. Colloid Interface Sci.* **1991**, *147*, 103–118. (c) Heiney, P. A.; Grüneberg, K.; Fang, J. *Langmuir* **2000**, *16*, 2651–2657. (d) Hooper, A. E.; Werho, D.; Hopson, T.; Palmer, O. *Surf. Interface Anal.* **2001**, *31*, 809–814.

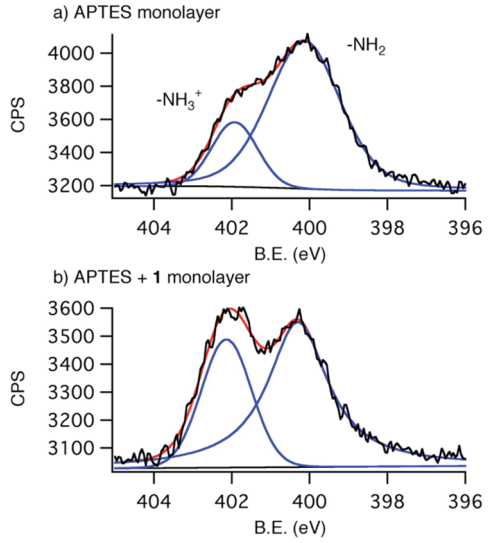

Figure 5. XPS spectrum for N1s region taken at the escape angle of 0°. (a) APTES monolayer. (b) APTES monolayer with **1** added to form a monolayer on top.

spectrum of N1s (escape angle 0°) of an APTES monolayer in the absence of **1**; there are two peaks that can be assigned to $-NH_2$ (400.1 eV) and $-NH_3^+$ (401.9 eV) in a ratio of 81:19. This is consistent with the previous report.[13d] After the monolayer of **1** is formed, the ratio of $-NH_2$ and $-NH_3^+$ peaks became 67:33 (Figure 5b), which implies the formation of a salt between the compound **1** and APTES monolayer. XPS spectrum of the monolayer of **2** gave essentially the same result (Supporting Information Figure S-11). In addition, the ratio of Fe and C (Fe/C = 1.3×10^{-2}) decreased when the spectrum was taken with the escape angle of 75° (Fe/C = 7.4×10^{-3}) which in turn suggest the upright orientation of the compound **2** on the surface.

Infrared spectroscopy yielded further chemical information about the interface of the monolayer of **1** and APTES. The C═O stretch of pure **1** (1701 cm^{-1}, Figure 6a) disappeared in the spectrum of the monolayer (Figure 6b). Instead, asymmetric and symmetric stretching modes of carboxylate CO_2^- (1608 and 1396 cm^{-1}, respectively) became predominant, which suggests that **1** is attached to the amine surface through hydrogen bonding. The differential spectrum in which the amine surface spectrum was subtracted from the monolayer spectrum, showed a small amount of C═O stretch remaining (Figure 7). This might be attributed to a residual amount of the carboxylic acids that are not hydrogen bonded to the APTES, or to occasional molecules that are sitting in alternative orientation (lying on the side or standing upside down). Even so, the major resonances are CO_2^- stretches, which suggest the predominant upright orientation for **1**. The monolayer spectrum of **2** is essentially the same (Supporting Information Figure S-12 and 13).

Monolayers of both **1** and **2** are very stable; the UV−vis spectrum did not show significant change over several weeks under air or more than 15 h under argon at 300 °C. Compared with the monolayer of C_{60} pentabiphenyl derivative ($C_{60}(C_6H_4C_6H_4{-}COOH)_5Me$) on gold,[7d]

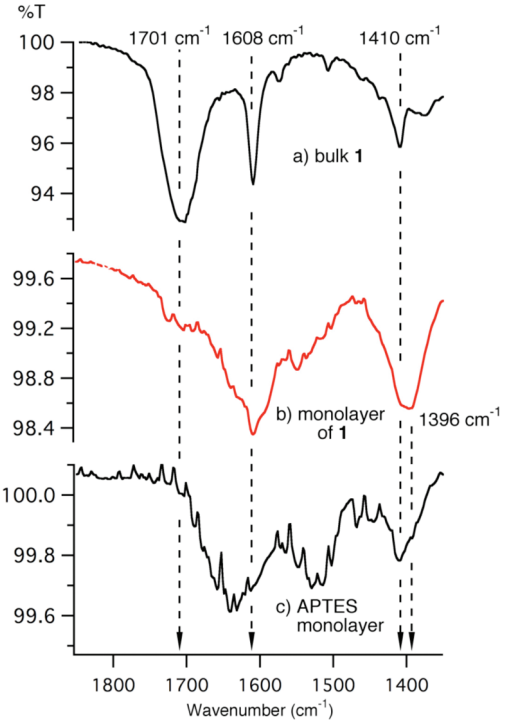

Figure 6. Carbonyl region of the IR spectrum of the (a) bulk **1**, (b) monolayer of **1** on APTES monolayer, and (c) APTES monolayer.

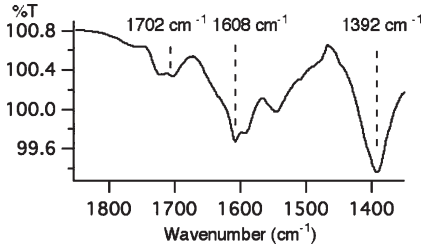

Figure 7. Differential IR spectrum of the monolayer of **1** subtracted with the spectrum of APTES monolayer.

the coverage 0.42 molecules/nm^2 for the monolayer of **1** and 0.50 molecules/nm^2 for the monolayer of **2** is quite reasonable (0.40 molecules/nm^2 for pentabiphenyl derivative). It is interesting to note that the pentabiphenyl derivative stands upright on bare gold surface without any adhesion layer under in situ STM conditions. To explore the utility of these monolayers, we will show examples of both *n*-type and *p*-type transistors using the monolayers as a functionalized insulating layer.

First SAMs of **1** and **2** were tested to see their effects on *n*-type FETs made from C_{60}. Au/Cr electrodes were deposited (5 nm Cr followed by 50 nm Au) through a shadow mask by thermal evaporation onto a silicon wafer that has a 300 nm oxide layer as an insulator, then the monolayer of either **1** or **2** was assembled on top of this substrate. The channel length was 10 μm and the electrode width was 115 μm. C_{60} was then thermally evaporated onto the substrate (1.5−1.7 Å/s at $<10^{-6}$ Torr, C_{60} layer thickness: 50 nm). The measurement was carried out in a glovebox without exposing the device to air. The output of the resulting transistor is shown in Figure 8b. With a monolayer of **1**, the mobility was μ = 0.02 $cm^2\ V^{-1}\ s^{-1}$, which is quite typical for C_{60}

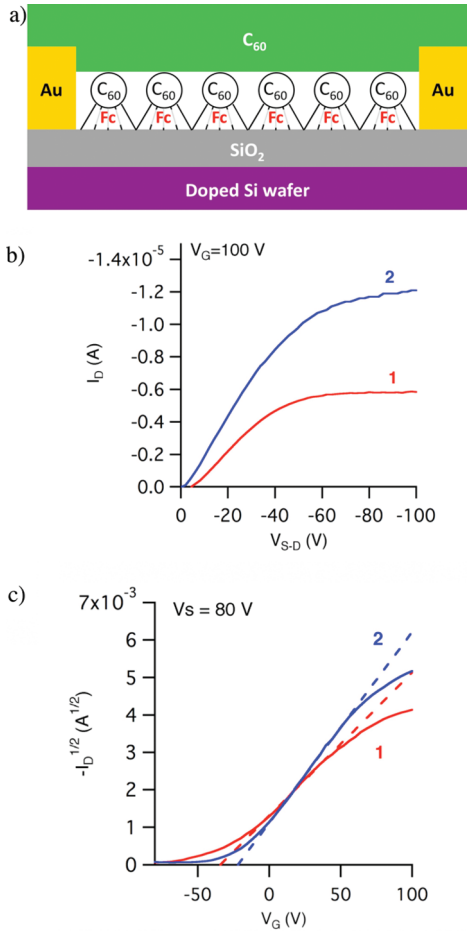

Figure 8. (a) Schematic illustration of an FET fabricated for C_{60} transistors. Fc: ferrocene. (b) Transistor output for C_{60} transistors with the monolayer of **1**, **2**. (c) Transconductance: The dotted lines are a fit of the linear portion of the data points. The source-drain voltage $V_{S\text{-}D}$ was held at 80 V.

FETs.[3c] With a monolayer of **2** the mobility was increased to $\mu = 0.04\ cm^2\ V^{-1}\ s^{-1}$, which is twice as high as with the monolayer of **1**. The difference is attributable to the ferrocene moiety: since C_{60} is an electron acceptor and ferrocene is an electron donor, carrier generation is more efficient in the presence of ferrocene than in its absence. The threshold voltage was −34 V in the case of **1** and −22 V for **2**. This is a large shift from the typical value, which is >0 V. An aligned dipole layer generated by the salt of amine and carboxylic acid at the interface of **1** (or **2**) and APTES monolayer could be responsible for the shift of the threshold voltage.[14]

Recently, we reported that the contorted hexabenzocoronene (HBC), **3**, shows good performance in spuncoat OFETs.[9] The effect of monolayers of **1** and **2** in the FETs using **3** was investigated. Beneficial intermolecular interactions can be expected in these pairings, not only because C_{60} is an electron acceptor and HBC is a donor but also because their shapes, a ball and a socket, respectively, are complementary (Figure 9).[15]

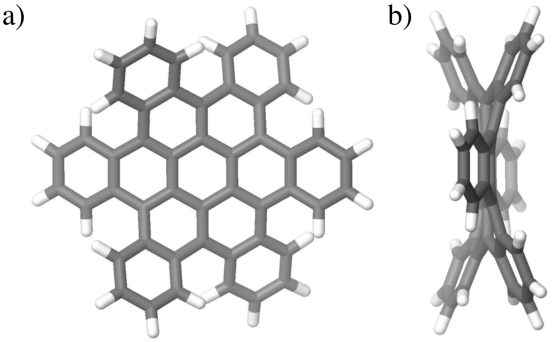

Figure 9. Structure of contorted hexabenzocoronene. (a) Front view. (b) Side view.

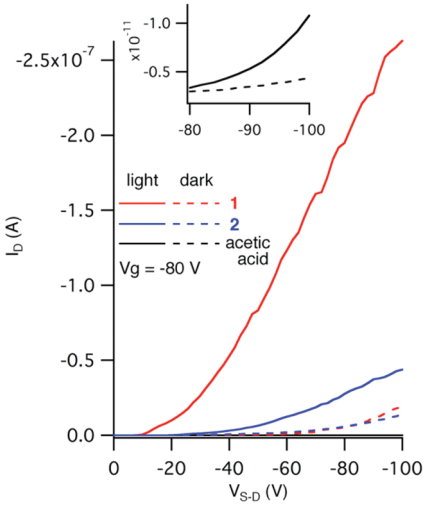

Figure 10. Transistor output of HBC **3** with different kinds of monolayer. Inset is the out put for the transistors with acetic acid monolayer.

The device was fabricated as follows. Au/Cr electrodes were evaporated (5 nm Cr followed by 50 nm Au) through a shadow mask onto the silicon wafer, which has 300 nm oxide layer as an insulator. The channel was 85 μm long and 2 mm wide. Then the solution of **3** was spuncoat onto the SAMs of **1** or **2**. The transistor output is shown in Figure 10. When the measurement was carried out in the dark, two devices showed similar characteristics (dotted lines); however, when the measurement was carried out in the ambient light, we found an interesting change: the transistor incorporating **1** had higher current than the one with **2**. The light−dark current ratio (I_D(light)/I_D(dark)) at $V_{S\text{-}D} = -100$ V was 14 for the former and 3 for the latter. We measured a similar OFET that used an acetic acid layer[16] instead of **1** (or **2**). Although it had negligible current either with or without light, the light−dark current ratio at $V_{S\text{-}D} = -100$ V was 2.5, which is similar to the FET with

(14) (a) Kobayashi, S.; Nishikawa, T.; Takenobu, T.; Mori, S.; Shimoda, T.; Mitani, T.; Shimotani, H.; Yoshimoto, N.; Ogawa, S.; Iwasa, Y. *Nat. Mater.* **2004**, *3*, 317–322. (b) Takeya, J.; Nishikawa, T.; Takenobu, T.; Kobayashi, S.; Iwasa, Y.; Mitani, T.; Goldmann, C.; Krellner, C.; Batlogg, B. *Appl. Phys. Lett.* **2004**, *85*, 5078–5080.

(15) Tremblay, N. J.; Gorodetsky, A. A.; Cox, M. P.; Schiros, T.; Kim, B.; Steiner, R.; Bullard, Z.; Sattler, A.; So, W.-Y.; Itoh, Y.; Toney, M. F.; Ogasawara, H.; Ramirez, A. P.; Kymissis, I.; Steigerwald, M. L.; Nuckolls, C. *ChemPhysChem* **2010**, *11*, 799–803.

(16) Acetic acid layer was prepared using the same method as for the preparation of the monolayer of **1** and **2**. The concentration of the acetic acid solution was five times higher than the solution of **1** and **2** to make the concentration of the "acid" (number of the −COOH group) same. We consider that the acetic acid makes a salt on APTES surface which prevents from evaporation.

the monolayer of **2**. Thus the behavior of the monolayer/HBC devices can be explained by the photoinduced charge transfer between C_{60} moiety of the monolayer and the HBC.[8h,17] The lower current with the monolayer of **2** could be attributed to the electron-donating ferrocene. Charge transfer from HBC might be suppressed by ferrocene which leads to ineffective channel formation by light.

Conclusion

We have demonstrated the formation of uniform monolayers of the compounds **1** and **2** on silicon oxide surfaces with a straightforward method that involves dipping the amino-terminated surface into the solution of the C_{60} derivatives. This does not require any covalent modification of C_{60} on the surface, which could potentially result in a nonuniform modification of the C_{60} molecules resulting in a surface of a nonuniform electronic structure. The monolayer could be used for the surface modification of the insulating layer of OFETs. When C_{60} was used as a semiconducting layer in an OFET, the mobility when **1** was used was 0.02 $cm^2\ V^{-1}\ s^{-1}$. This value doubles in the presence of the monolayer of **2**, indicating the efficient channel formation by electron donating ferrocene moiety. A more surprising fact is the generation of photocurrent in the presence of contorted HBC, **3**. Both the donor−acceptor interaction and the geometrical ball−socket interaction apparently play important roles in the photocurrent generation.[15]

Acknowledgment. We thank Dr. Alian Adnot in Université Laval for XPS measurement. This work was generously supported by MEXT, Japan (KAKENHI to E.N., 22000008). Y.I. thanks the Japan Society for the Promotion of Science (JSPS) for a Research Fellow ship for Young Scientises (18·9971). Use of the National Synchrotron Light Source, Brookhaven National Laboratory, was supported by the U.S. Department of Energy, Office of Science, Office of Basic Energy Sciences, under Contract No. DE-AC02-98CH10886. The authors would like to thank M. Fukuto and H. Zhou from National Synchrotron Light Source for fruitful discussions.

Supporting Information Available: UV−vis spectra of the compound **1** and **2** both for the solution and the monolayer, AFM images for the monolayer of **1** and **2**, model parameters for X-ray reflectivity, survey spectra of XPS analysis of the monolayer of **1** and **2**, the high resolution scan for N1s region of the monolayer of **2**, IR spectrum of the compound **2** both for bulk and the monolayer, and details of the OFETs properties. This material is available free of charge via the Internet at http://pubs.acs.org.

(17) Yamamoto, Y.; Zhang, G.; Jin, W.; Fukushima, T.; Ishii, N.; Saeki, A.; Seki, S.; Tagawa, S.; Minari, T.; Tsukagoshi, K.; Aida, T. *Proc. Natl. Acad. Sci. U.S.A.* **2009**, *106*, 21051–21056.